

Adaptive Sampling of Pareto Frontiers with Binary Constraints Using Regression and Classification

Raoul Heese, Michael Bortz

Fraunhofer Center for Machine Learning

Fraunhofer-Institut für Techno- und Wirtschaftsmathematik ITWM

Fraunhofer-Platz 1, 67663 Kaiserslautern, Germany

{raoul.heese, michael.bortz}@itwm.fraunhofer.de

Abstract—We present a novel adaptive optimization algorithm for black-box multi-objective optimization problems with binary constraints on the foundation of Bayes optimization. Our method is based on probabilistic regression and classification models, which act as a surrogate for the optimization goals and allow us to suggest multiple design points at once in each iteration. The proposed acquisition function is intuitively understandable and can be tuned to the demands of the problems at hand. We also present a novel ellipsoid truncation method to speed up the expected hypervolume calculation in a straightforward way for regression models with a normal probability density. We benchmark our approach with an evolutionary algorithm on multiple test problems.

Index Terms—Bayes optimization, adaptive sampling, regression, classification, probabilistic models, constraints, feasibility

I. INTRODUCTION

Bayesian optimization is a derivative-free strategy for the global optimization of computationally expensive black-box functions [1]. The basic idea is to build a surrogate for the objective function and to define an acquisition function based on this surrogate to decide where to sample next in an iterative approach. Ideally, a good compromise between the number of evaluations and the approximation quality of the solution can be found. Real-world optimization problems can also involve black-box constraints [2] which restrict the solution space.

Multi-objective optimization (MOO) problems require the simultaneous optimization of more than one objective function [3], [4]. Specifically, we consider MOO problems \mathcal{O} of the form

$$\begin{aligned} & \underset{\mathbf{x}}{\text{minimize}} && \mathbf{y} \equiv \mathbf{y}(\mathbf{x}) \equiv (y_1(\mathbf{x}), \dots, y_n(\mathbf{x})) \\ & \text{subject to} && f \equiv f(\mathbf{x}) = \text{feasible} \\ & \text{where} && \mathbf{x} \in \mathcal{X} \subseteq \mathbb{R}^d \text{ (design variables)} \\ & && \mathbf{y} \in \mathcal{Y} \subseteq \mathbb{R}^n \text{ (objectives)} \\ & && f \in \mathcal{F} \equiv \{\text{feasible, infeasible}\} \end{aligned} \quad (1)$$

which also involve binary constraints $f(x)$.

For a non-trivial MOO problem there is no solution that allows an independent optimization of all objectives. Instead, trade-offs between two or more conflicting objectives have to be taken into account. In other words, there exist a set of Pareto optimal solutions for which none of the objective functions can

be decreased without increasing another. We write $\mathbf{y} \preceq \mathbf{y}'$ to state that $\mathbf{y} \in \mathcal{Y}$ dominates $\mathbf{y}' \in \mathcal{Y}$, which means that

$$\mathbf{y} \preceq \mathbf{y}' \Leftrightarrow y_i \leq y'_i \forall i = 1, \dots, n \wedge \mathbf{y} \neq \mathbf{y}'. \quad (2)$$

The full set of Pareto optimal objectives

$$\begin{aligned} \mathbf{P}(\mathcal{X}, \mathbf{y}(\mathbf{x}), f(\mathbf{x})) &\equiv \{\mathbf{y} \in \mathcal{Y} \mid \exists \mathbf{x} \in \mathcal{X} : \mathbf{y} = \mathbf{y}(\mathbf{x}) \\ &\wedge f(\mathbf{x}) = \text{feasible} \wedge \mathbf{y}' \not\preceq \mathbf{y} \forall \mathbf{x}' \in \mathcal{X} \setminus \{\mathbf{x}\} : \mathbf{y}' = \mathbf{y}(\mathbf{x}') \\ &\wedge f(\mathbf{x}') = \text{feasible}\} \end{aligned} \quad (3)$$

consequently represents the solution of (1) and is also known as the Pareto frontier of the MOO problem.

Thus, our goal is to approximate this Pareto frontier as accurately as possible with as few evaluations

$$\mathbf{S}(\mathbf{x}) \equiv (\mathbf{y}(\mathbf{x}), f(\mathbf{x})) = (\mathbf{y}, f) \quad (4)$$

as possible. This function can, for example, represent a complex simulation with a very long runtime that does not converge at certain design points, which leads to an infeasible outcome. In particular, we assume to have no knowledge about the inner structure of $\mathbf{S}(\mathbf{x})$ and can only evaluate it in the sense of a black-box.

In this manuscript, we first present a novel method of adaptive optimization to solve such kind of problems. Subsequently, we benchmark our algorithm. Finally, we close with a short summary.

II. PROPOSED METHOD

As sketched in Fig. 1, our proposed method of *adaptive optimization* consists of three consecutive steps in the spirit of a typical Bayesian optimization loop, which repeats until a certain stopping criterion is reached. First, two machine learning models are trained which form a surrogate for $\mathbf{S}(\mathbf{x})$, (4). Second, a model-dependent acquisition function $\text{AF}(\mathbf{x})$ is maximized to obtain a design point of interest \mathbf{x}_1 . This maximization may be repeated N_{seq} times to obtain a sequence of design points $\mathbf{x}_1, \mathbf{x}_2, \dots$, where the acquisition function is changed each time based on the previously obtained maximization results. And third, the sequence of design points is evaluated using $\mathbf{S}(\mathbf{x}_1), \mathbf{S}(\mathbf{x}_2), \dots$. A parallelized evaluation allows to reduce the total effective runtime of the algorithm in comparison with a single suggestion. In this sense, we approximate the Pareto frontier by adding new samples to our data set in each iteration. We have already demonstrated

that a related approach can be used to explore the feasibility regions of a design space [5]. A Python implementation of our proposed method is provided in [6].

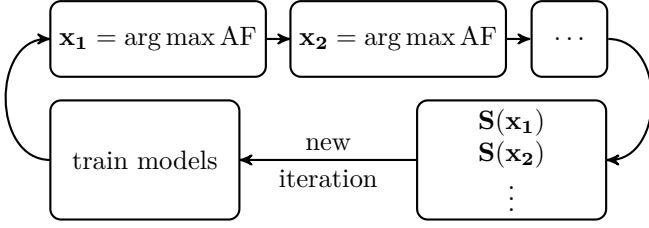


Figure 1: Basic sketch of our adaptive optimization method which works along the lines of the well-known Bayesian optimization loop. First, the machine learning models, (6), are updated based on the currently available data. Second, a model-dependent acquisition function AF , (8), is maximized iteratively to obtain the design points $\mathbf{x}_1, \mathbf{x}_2, \dots$, which are then evaluated using (4). For each maximization result, the acquisition function is changed based on the previous outcomes so that the following maximization will yield a different result. Finally, the loop may repeat again until a certain stopping criterion is reached. Our approach allows a parallelized evaluation of N_{seq} simulations, which leads to a significant reduction of the effective runtime.

A. Models

Each evaluation of (4) yields a data point $\mathbf{d} \equiv (\mathbf{x}, \mathbf{y}, f)$ and the set of k of such data points is denoted as the data set

$$\mathbf{D} \equiv \{\mathbf{d}_1, \dots, \mathbf{d}_k\} \quad (5a)$$

in the data space \mathcal{D} . Note that we use bold indices to iterate vector-valued elements of a set, and non-bold indices to indicate the respective vector components. Furthermore, we use subscripts and superscripts to denote the partial data sets

$$\begin{aligned} \mathbf{D}_{\mathbf{x}} &\equiv \{\mathbf{x} \mid \forall (\mathbf{x}, \mathbf{y}, f) \in \mathbf{D}\} \\ \mathbf{D}_{\mathbf{y}}^* &\equiv \{\mathbf{y} \mid \forall (\mathbf{x}, \mathbf{y}, f) \in \mathbf{D} \mid f = \text{feasible}\} \\ \mathbf{D}_{\mathbf{xy}}^* &\equiv \{(\mathbf{x}, \mathbf{y}) \mid \forall (\mathbf{x}, \mathbf{y}, f) \in \mathbf{D} \mid f = \text{feasible}\} \\ \mathbf{D}_{\mathbf{xf}} &\equiv \{(\mathbf{x}, f) \mid \forall (\mathbf{x}, \mathbf{y}, f) \in \mathbf{D}\} \end{aligned} \quad (5b)$$

with respect to \mathbf{D} .

To approximate (4) based on \mathbf{D} we define two machine learning models. First, a probabilistic regression model

$$\hat{p}_y(\mathbf{y} | \mathbf{D}_{\mathbf{xy}}^*, \mathbf{x}) : \mathcal{Y} \times \mathcal{D} \times \mathcal{X} \mapsto \mathbb{R}_{\geq 0}, \quad (6a)$$

which predicts the probability density \hat{p}_y of $\mathbf{S}(\mathbf{x})$ yielding the objectives \mathbf{y} . It is trained only on the feasible data points, whereas infeasible data points are ignored. Second, a probabilistic classification model

$$\hat{p}_f(f | \mathbf{D}_{\mathbf{xf}}, \mathbf{x}) : \mathcal{F} \times \mathcal{D} \times \mathcal{X} \mapsto [0, 1], \quad (6b)$$

which predicts the probability \hat{p}_f that evaluating $\mathbf{S}(\mathbf{x})$ leads to a feasibility f and is trained on both feasible and infeasible data points.

These two models allow us to determine the expected optimization goal

$$\hat{\mathbf{y}}(\mathbf{D}_{\mathbf{xy}}^*, \mathbf{x}) \equiv \int_{-\infty}^{\infty} \mathbf{y} \hat{p}_y(\mathbf{y} | \mathbf{D}_{\mathbf{xy}}^*, \mathbf{x}) d\mathbf{y} \quad (7a)$$

and the expected feasibility

$$\hat{f}(\mathbf{D}_{\mathbf{xf}}, \mathbf{x}) \equiv \sum_{f \in \mathcal{F}} f \hat{p}_f(f | \mathbf{D}_{\mathbf{xf}}, \mathbf{x}), \quad (7b)$$

respectively, which together represent a surrogate for (4). For Bayes optimization one usually uses Gaussian process regression to model the objectives. For our method, however, any probabilistic regression model can be applied. For example, in section III we demonstrate the use of a Bayesian ridge regression model.

B. Acquisition function

Our model-dependent acquisition function

$$\begin{aligned} AF(\mathbf{x}) &\equiv U(\mathbf{w}, \mathbf{D}, \mathbf{y}_{\text{ref}}, \gamma, \delta; \mathbf{x}) \\ &\equiv \frac{w_{\text{opt}}}{|\mathbf{w}|_1} U_{\text{opt}}(\mathbf{D}, \mathbf{y}_{\text{ref}}, \gamma; \mathbf{x}) + \frac{w_{\text{con}}}{|\mathbf{w}|_1} U_{\text{con}}(\mathbf{D}; \mathbf{x}) \\ &\quad + \frac{w_{\text{exp}}}{|\mathbf{w}|_1} U_{\text{exp}}(\mathbf{D}, \delta; \mathbf{x}) \in [0, 1] \end{aligned} \quad (8)$$

consists of three parts, the influence of which can be controlled by the choice of the weights $\mathbf{w} \equiv (w_{\text{opt}}, w_{\text{con}}, w_{\text{exp}}) \geq 0$.

The optimization part U_{opt} ensures that the suggested design points improve the Pareto frontier within the feasible region, whereas the constraint-finding part U_{con} chooses points close to the border between feasible and infeasible domains to improve the classification model. Finally, the exploration part U_{exp} leads to a spreading of points in the design space and hence promotes an exploration of unknown regions. Summarized, (8) can be understood as an *expected utility* of a design point \mathbf{x} which takes all of the previously mentioned effects into account and tries to balance exploration and exploitation by the means of the chosen weights \mathbf{w} . In the following, we explain the three utility components in more detail.

1) *Optimization part:* The optimization utility

$$\begin{aligned} U_{\text{opt}}(\mathbf{D}, \mathbf{y}_{\text{ref}}, \gamma; \mathbf{x}) &\equiv \hat{p}_f(f = \text{feasible} | \mathbf{D}_{\mathbf{xf}}, \mathbf{x}) \\ &\quad \times O(\mathbf{D}, \mathbf{y}_{\text{ref}}, \gamma; \mathbf{x}), \end{aligned} \quad (9)$$

consists of a product of two terms. The first term is based on the classification model, (6b), and corresponds to the predicted probability of a feasible outcome when evaluating \mathbf{x} . It acts as a weighting factor for the second term

$$O(\mathbf{D}, \mathbf{y}_{\text{ref}}, \gamma; \mathbf{x}) \equiv 1 - \exp \left[\gamma \frac{\text{EVI}(\mathbf{D}_{\mathbf{xy}}^*, \mathbf{y}_{\text{ref}}; \mathbf{x})}{-\Gamma(\mathbf{D}_{\mathbf{y}}^*, \mathbf{y}_{\text{ref}})} \right], \quad (10)$$

which is a measure for the expected improvement of the Pareto frontier. It contains the user-defined parameter $\gamma \in \mathbb{R}_{>0}$ and the relative volume

$$\Gamma(\mathbf{D}_{\mathbf{y}}^*, \mathbf{y}_{\text{ref}}) \equiv \prod_{i=1}^n \max_{\mathbf{y} \in \mathbf{P}(\mathbf{D}_{\mathbf{y}}^*)} (y_{\text{ref},i} - y_i), \quad (11)$$

which both act as rescaling factors to the expected Pareto volume improvement

$$\text{EVI}(\mathbf{D}_{\mathbf{xy}}^*, \mathbf{y}_{\text{ref}}; \mathbf{x}) \equiv \int_{-\infty}^{+\infty} \Delta V(\mathbf{D}_{\mathbf{y}}^*, \mathbf{y}_{\text{ref}}; \mathbf{y}) \times \hat{p}_y(\mathbf{y} | \mathbf{D}_{\mathbf{xy}}^*, \mathbf{x}) d\mathbf{y} \quad (12)$$

with

$$\Delta V(\mathbf{D}_{\mathbf{y}}^*, \mathbf{y}_{\text{ref}}; \mathbf{y}) \equiv V(\mathbf{D}_{\mathbf{y}}^* \cup \{\mathbf{y}\}, \mathbf{y}_{\text{ref}}) - V(\mathbf{D}_{\mathbf{y}}^*, \mathbf{y}_{\text{ref}}), \quad (13)$$

where we have recalled the regression model, (6a). Hence, (12) represents the expected increase of the Pareto volume

$$V(\mathbf{D}_{\mathbf{y}}^*, \mathbf{y}_{\text{ref}}) \equiv \text{Vol}(\{\mathbf{y} \in \mathbb{R}^n \mid \mathbf{P}(\mathbf{D}_{\mathbf{y}}^*) \preceq \mathbf{y} \preceq \mathbf{y}_{\text{ref}}\}) \quad (14)$$

with respect to a given reference point

$$\mathbf{y}_{\text{ref}} \equiv (y_{\text{ref},1}, \dots, y_{\text{ref},n}) \in \mathbb{R}^n \quad (15)$$

when the point $\mathbf{y} \in \mathcal{Y}$ is added to the existing data set $\mathbf{D}_{\mathbf{y}}^*$. Here we make use of the Pareto optimal subset

$$\mathbf{P}(\mathbf{D}_{\mathbf{y}}^*) \equiv \{\mathbf{y} \in \mathbf{D}_{\mathbf{y}}^* \mid \mathbf{y}' \not\preceq \mathbf{y} \forall \mathbf{y}' \in \mathbf{D}_{\mathbf{y}}^* \setminus \{\mathbf{y}\}\} \subseteq \mathbf{D}_{\mathbf{y}}^*, \quad (16)$$

which is defined in analogy to (3). In appendix A we outline how (12) can be expressed in a closed form for a regression model with a normal probability density.

The expected Pareto volume improvement does not take the feasibility of the problem into account since the regression model assumes that all predicted points are feasible. However, the first factor in (9), compensates this defect so that U_{opt} describes the expected improvement of the Pareto frontier weighted by the probability of the outcome being feasible.

2) *Constraint-finding part*: The constraint-finding utility

$$U_{\text{con}}(\mathbf{D}; \mathbf{x}) \equiv p_{\not\preceq}(\mathbf{D}_{\mathbf{xy}}^*; \mathbf{x}) S(\hat{p}_f(f = \text{feasible} | \mathbf{D}_{\mathbf{xf}}, \mathbf{x})) \quad (17)$$

also consists of a product of two terms. The first term

$$p_{\not\preceq}(\mathbf{D}_{\mathbf{xy}}^*; \mathbf{x}) \equiv p(\hat{\mathbf{y}}(\mathbf{D}_{\mathbf{xy}}^*; \mathbf{x}) \not\preceq \mathbf{y} \forall \mathbf{y} \in \mathbf{D}_{\mathbf{y}}^*) \quad (18)$$

represents the probability that the expected optimization goal $\hat{\mathbf{y}}(\mathbf{D}_{\mathbf{xy}}^*; \mathbf{x})$, (7a), is not being dominated by the points in the already explored data set $\mathbf{D}_{\mathbf{y}}^*$. This probability can be expressed in a closed form for a regression model with a normal probability density as we outline in appendix C. Equation (18) acts as a weighting factor for the second term in (17), which represents the Shannon information entropy of a binary event

$$S(p) \equiv \frac{-p \ln p - (1-p) \ln(1-p)}{\ln 2} \quad (19)$$

for the predicted probability of a feasible outcome, (6b).

$S(p)$ attains its only maximum for $p = \frac{1}{2}$ so that the points with the highest predicted uncertainty are assigned the largest utility. The first term weights this value with the probability of the predicted objective being non-dominated so that design points which lead to expectably dominated predictions end up with a vanishing utility. U_{con} consequently describes the feasibility uncertainty weighted by the probability of the outcome not being dominated by already explored points.

3) *Explorative part*: The explorative utility

$$U_{\text{exp}}(\mathbf{D}, \mathcal{K}; \mathbf{x}) \equiv p_{\not\preceq}(\mathbf{D}_{\mathbf{xy}}^*; \mathbf{x}) R(\mathbf{D}_{\mathbf{x}}, \delta; \mathbf{x}) \quad (20)$$

is again a product of two terms. The first term is the probability of the predicted objective being non-dominated, (18). The second term represents the normalized repulsion

$$R(\mathbf{D}_{\mathbf{x}}, \delta; \mathbf{x}) \equiv \frac{\max_{\mathbf{x}' \in \mathbf{D}_{\mathbf{x}}} \delta(\mathbf{x}, \mathbf{x}')}{\max_{\mathbf{x}', \mathbf{x}'' \in \mathcal{X}} \delta(\mathbf{x}', \mathbf{x}'')} \quad (21)$$

based on a user-defined distance metric

$$\delta : \mathcal{X} \times \mathcal{X} \mapsto \mathbb{R}_{\geq 0}. \quad (22)$$

The denominator in (21) is a constant with respect to \mathbf{x} and therefore just serves as a constant rescaling factor.

Equation (21) increases with an increasing distance of a design point \mathbf{x} to already explored design points in $\mathbf{D}_{\mathbf{x}}$. Hence, U_{expl} describes the point sparsity weighted by the probability of the outcome not being dominated by already explored points.

C. Ellipsoid truncation method

For our proposed method we have to repeatedly solve global optimization problems of the form

$$\mathbf{x}_{\mathbf{k}} \equiv \arg \max_{\mathbf{x} \in \mathcal{X}} U(\mathbf{w}, \mathbf{D}, \mathbf{y}_{\text{ref}}, \gamma; \delta; \mathbf{x}) \quad (23)$$

to find the next point $\mathbf{x}_{\mathbf{k}}$. Since global optimization strategies can not guarantee an optimal solution, a suitable compromise between a high utility outcome and a low calculation time has to be found. In other words, since a numerical optimization result is an approximation, we can as well approximate the utility function to reduce computational effort. In appendix B we present the *ellipsoid truncation method* as an approximation for the expected Pareto volume improvement $\text{EVI} \approx \widetilde{\text{EVI}}$, (12), which can be applied for regression models with a normal probability density. The basic idea is to truncate all terms of little effect based on an intersection of the non-dominated regions with an ellipse centered at the predicted mean with an eccentricity proportional to the predicted standard deviation and the user-defined approximation control parameter $\sigma_{\text{ref}} \in \mathbb{R}_{>0}$. Then

$$\begin{aligned} U_{\text{opt}}(\mathbf{D}, \mathbf{y}_{\text{ref}}, \gamma; \mathbf{x}) &\approx \widetilde{U}_{\text{opt}}(\mathbf{D}, \mathbf{y}_{\text{ref}}, \sigma_{\text{ref}}, \gamma; \mathbf{x}) \\ &\equiv \hat{p}_f(f = \text{feasible} | \mathbf{D}_{\mathbf{xf}}, \mathbf{x}) \\ &\times \left\{ 1 - \exp \left[\gamma \frac{\widetilde{\text{EVI}}(\mathbf{D}_{\mathbf{xy}}^*, \mathbf{y}_{\text{ref}}, \sigma_{\text{ref}}; \mathbf{x})}{-\Gamma(\mathbf{D}_{\mathbf{y}}^*, \mathbf{y}_{\text{ref}})} \right] \right\} \end{aligned} \quad (24)$$

corresponds to an approximation $\widetilde{\mathbf{x}}_{\mathbf{k}}(\sigma_{\text{ref}}) \approx \mathbf{x}_{\mathbf{k}}$ of the originally proposed expression, (23), with $\widetilde{\mathbf{x}}_{\mathbf{k}}(\sigma_{\text{ref}} \rightarrow \infty) \rightarrow \mathbf{x}_{\mathbf{k}}$.

D. Algorithm

Algorithm 1 represents our proposed optimization method as sketched in Fig. 1. It contains the following functions:

- **OPTIMIZE**($\mathcal{O}, N_{\text{seq}}$): Solve the black-box optimization task \mathcal{O} , (1), using design point sequences of length $N_{\text{seq}} \geq 1$. Return the resulting data set of pareto points, (16), as an approximation of the true Pareto frontier, (3).

- **INITIALCALCULATION**(\mathcal{X}, \mathbf{S}): Calculate an initial set of randomly chosen points on \mathcal{X} using \mathbf{S} , (4), and return the resulting data set \mathbf{D} , (5),
- **STOP**(\mathbf{D}): Check whether a predefined stopping criterion is fulfilled (usually based on \mathbf{D} , e. g., a maximum number of sampled points) and return the boolean outcome.
- **UPDATERMODELS**(\mathbf{D}): Train the machine learning models \mathbf{M} , (6), based on \mathbf{D} and return them.
- **SUGGESTION**($\mathcal{X}, \mathbf{M}, \mathbf{D}'$): Maximize the approximated utility function, (8) and (24). The utility function is calculated using the machine learning models \mathbf{M} , (6), and the data set \mathbf{D}' . Return the resulting design point \mathbf{x} .
- **PREDICTION**(\mathbf{M}, \mathbf{x}): Evaluate the expectation values of the models \mathbf{M} at the design point \mathbf{x} . Return both the expected objectives $\hat{\mathbf{y}}$, (7a), and the expected feasibility \hat{f} , (7b).
- **CALCULATION**($\mathbf{S}, \mathbf{D}'_{\mathbf{x}}$): Evaluate \mathbf{S} for new design points $\mathbf{x} \in \mathbf{D}'_{\mathbf{x}}$. Suggested points can be evaluated in parallel to reduce calculation time. Return the data set of results.
- **PARETO**($\mathbf{D}_{\mathbf{y}}^*$): Return the Pareto optimal subset of $\mathbf{D}_{\mathbf{y}}^*$, (16).

Algorithm 1 Adaptive optimization algorithm

```

1: function OPTIMIZE( $\mathcal{O}, N_{\text{seq}}$ )
2:    $\mathbf{D} \leftarrow \text{INITIALCALCULATION}(\mathcal{X}, \mathbf{S})$ 
3:   while not STOP( $\mathbf{D}$ ) do
4:      $\mathbf{M} \leftarrow \text{UPDATERMODELS}(\mathbf{D})$ 
5:      $\mathbf{D}' \leftarrow \mathbf{D}$ 
6:      $\nu \leftarrow 0$ 
7:     while  $\nu < N_{\text{seq}}$  do
8:        $\mathbf{x} \leftarrow \text{SUGGESTION}(\mathcal{X}, \mathbf{M}, \mathbf{D}')$ 
9:        $\hat{\mathbf{y}}, \hat{f} \leftarrow \text{PREDICTION}(\mathbf{M}, \mathbf{x})$ 
10:       $\mathbf{D}' \leftarrow \mathbf{D}' \cup \{(\mathbf{x}, \hat{\mathbf{y}}, \hat{f})\}$ 
11:       $\nu \leftarrow \nu + 1$ 
12:    end while
13:     $\mathbf{D} \leftarrow \mathbf{D} \cup \text{CALCULATION}(\mathbf{S}, \mathbf{D}'_{\mathbf{x}})$ 
14:  end while
15:  return PARETO( $\mathbf{D}_{\mathbf{y}}^*$ )
16: end function

```

III. BENCHMARK

In this section, we evaluate the performance of our proposed adaptive optimization algorithm `adaptive` and compare it to the evolutionary algorithm `nasgairi` [12]. Specifically, we study the six different benchmark problems listed in Tab. I, five of which are also sketched in Fig. 2. They are all in the form of (1). Although we show constraints $\mathbf{c}(\mathbf{x})$ for each problem, we effectively use only the resulting binary feasibility

$$f(\mathbf{x}) = \begin{cases} \text{feasible} & \text{if } c_i(\mathbf{x}) \leq 0 \forall i = 1, \dots, m \\ \text{infeasible} & \text{else} \end{cases} \quad (25)$$

as the mutual fulfillment condition of all m constraints. In other words, we assume that the constraints are not accessible and we can only observe f . The Pareto frontiers of the problems CEX, FFF and CIR are disjointed in the design space

and additionally disjointed in the objective space for the former two.

Initially, we randomly choose N_0 design points which are uniformly distributed on an initial design space $\mathcal{X}_0 \subseteq \mathcal{X}$. The resulting initial data set is then fed to the competing algorithms such that each candidate has the same initial information about the problem. For `nasgairi` we choose a constant population size of 50. The options for our proposed method are shown in the last column of Tab. I. We write `adaptive-1` for the choice $N_{\text{seq}} = 1$ and `adaptive-5` for $N_{\text{seq}} = 5$. As distance metric, (22), we use

$$\delta_{\epsilon, \mathcal{X}}(\mathbf{x}_1, \mathbf{x}_2) \equiv 1 - \exp[-\epsilon |\boldsymbol{\mu}_{\mathcal{X}}(\mathbf{x}_1) - \boldsymbol{\mu}_{\mathcal{X}}(\mathbf{x}_2)|_2^2] \quad (26)$$

based on the user-defined control parameter $\epsilon \geq 0$ and the scaling function

$$\boldsymbol{\mu}_{\mathcal{X}}(\mathbf{x}) \equiv \frac{\mathbf{x} - \mathbf{x}_{\min}(\mathcal{X})}{\mathbf{x}_{\max}(\mathcal{X}) - \mathbf{x}_{\min}(\mathcal{X})}, \quad (27a)$$

where

$$\mathbf{x}_{\min}(\mathcal{X}) \equiv \arg \min_{\mathbf{x} \in \mathcal{X}} \mathbf{x} \quad (27b)$$

and

$$\mathbf{x}_{\max}(\mathcal{X}) \equiv \arg \max_{\mathbf{x} \in \mathcal{X}} \mathbf{x}, \quad (27c)$$

respectively. This choice of metric is motivated by the feature space distance of an exponential kernel [13].

For the utility maximization, (23), we use a two step approach. First, we perform a differential evolution [14] and then use an L-BFGS-B optimizer [15] to further improve the result. The classification model, (6b), is realized with a RBF kernel support vector machine calibrated by Platt scaling and with hyperparameters optimized by cross-validation. For BNH, SRN, FFF, and CIR the regression model, (6a), is a Gaussian process regression with Matern kernel, whereas for OSY and CEX we choose a Bayesian ridge regression model with polynomial features.

A. Performane metrics

We use three different metrics to quantify the performance of the competing algorithms, which we explain in the following.

1) *Relative total dominated volume*: The approximation quality of the Pareto frontier can be quantified by the relative total dominated volume

$$\Delta V(\mathcal{O}, \mathbf{y}_{\text{ref}}, \text{alg}) \equiv \frac{V(\mathbf{D}_{\mathbf{y}}^*(\text{alg}), \mathbf{y}_{\text{ref}})}{V(\mathbf{P}(\mathcal{O}), \mathbf{y}_{\text{ref}})} \in [0, 1] \quad (28)$$

as a ratio between the estimated Pareto volume and the volume of the actual Pareto set, where we have recalled (14).

2) *Effective runtime*: We determine the pure runtime of the algorithm $T(\text{alg})$ from the start up to iteration $N_{\text{iter}}(\text{alg})$ excluding the time for the simulation evaluations, (4). Since for benchmark purposes we can freely choose an artificial evaluation time of the simulations to study different scenarios, we define that N_{sim} simulations can be evaluated in parallel during a constant runtime T_{sim} . Given an algorithm that suggests sequences of $N_{\text{seq}}(\text{alg})$ design points for each of $N_{\text{iter}}(\text{alg})$

Table I: Definitions of the test problems used for our benchmarks with the notation from (1) and (25) and section II. Five of the six problems are also sketched in Fig. 2.

Problem name and Ref.	Design space \mathcal{X}	Objectives $y(\mathbf{x})$	Constraints $c(\mathbf{x})$	Initial domain \mathcal{X}_0	Initial samples N_0	Reference point \mathbf{y}_{ref}	Adaptive optimization parameters
BNH [7]	$d = 2$ $x_1 \in [-5, 15]$ $x_2 \in [-10, 10]$	$n = 2$ $y_1(\mathbf{x}) = 4x_1^2 + 4x_2^2$ $y_2(\mathbf{x}) = (x_1 - 5)^2 + (x_2 - 5)^2$	$m = 2$ $c_1(\mathbf{x}) = (x_1 - 5)^2 + x_2^2 - 25$ $c_2(\mathbf{x}) = -(x_1 - 8)^2 - (x_2 + 3)^2 + 7.7$	$x_1 \in [0, 5]$ $x_2 \in [-5, 0]$	10	(200, 50)	$\mathbf{w} = (0, 1, 0)$ $\epsilon = 0$ $\gamma = 10$ $\sigma_{\text{ref}} = 1$
SRN [8]	$d = 2$ $x_1 \in [-20, 20]$ $x_2 \in [-20, 20]$	$n = 2$ $y_1(\mathbf{x}) = 2 + (x_1 - 2)^2 + (x_2 - 1)^2$ $y_2(\mathbf{x}) = 9x_1 - (x_2 - 1)^2$	$m = 2$ $c_1(\mathbf{x}) = x_1^2 + x_2^2 - 255$ $c_2(\mathbf{x}) = x_1 - 3x_2 + 10$	$x_1 \in [0, 20]$ $x_2 \in [0, 20]$	10	(250, 50)	$\mathbf{w} = (0, 1, 0)$ $\epsilon = 0$ $\gamma = 10$ $\sigma_{\text{ref}} = 1$
OSY [9]	$d = 6$ $x_1 \in [0, 10]$ $x_2 \in [0, 10]$ $x_3 \in [1, 5]$ $x_4 \in [0, 6]$ $x_5 \in [1, 5]$ $x_6 \in [0, 10]$	$n = 2$ $y_1(\mathbf{x}) = -25(x_1 - 2)^2 - (x_2 - 2)^2 \dots$ $\dots - (x_3 - 1)^2 - (x_4 - 4)^2 \dots$ $\dots - (x_5 - 1)^2$ $y_2(\mathbf{x}) = x_1^2 + x_2^2 + x_3^2 + x_4^2 + x_5^2 + x_6^2$	$m = 6$ $c_1(\mathbf{x}) = -x_1 - x_2 + 2$ $c_2(\mathbf{x}) = x_1 + x_2 - 6$ $c_3(\mathbf{x}) = x_2 - x_1 - 2$ $c_4(\mathbf{x}) = x_1 - 3x_2 - 2$ $c_5(\mathbf{x}) = (x_3 - 3)^2 + x_4 - 4$ $c_6(\mathbf{x}) = -(x_5 - 3)^2 - x_6 + 4$	$x_1 \in [2, 4]$ $x_2 \in [0, 3]$ $x_3 \in [2, 4]$ $x_4 \in [0, 2]$ $x_5 \in [1, 2]$ $x_6 \in [0, 10]$	100	(0, 80)	$\mathbf{w} = (0, 1, 0)$ $\epsilon = 0$ $\gamma = 200$ $\sigma_{\text{ref}} = 5$
CEX [10] (additional constraints)	$d = 2$ $x_1 \in [0.1, 1]$ $x_2 \in [0, 5]$	$n = 2$ $y_1(\mathbf{x}) = x_1$ $y_2(\mathbf{x}) = \frac{x_2 + 1}{x_1}$	$m = 4$ $c_1(\mathbf{x}) = -9x_1 - x_2 + 6$ $c_2(\mathbf{x}) = -9x_1 + x_2 + 1$ $c_3(\mathbf{x}) = .8 - x_1$ $c_4(\mathbf{x}) = x_1 - \frac{2}{3}$	$x_1 \in [1, 1]$ $x_2 \in [2.5, .5]$	10	(1, 9)	$\mathbf{w} = (1, 3, 1)$ $\epsilon = 1$ $\gamma = 1$ $\sigma_{\text{ref}} = 1.5$
FFF [11] (additional constraints)	$d = 2$ $x_1 \in [-1, 1]$ $x_2 \in [-1, 1]$	$n = 2$ $y_1(\mathbf{x}) = 1 - \exp \left[-\left(x_1 - \frac{1}{\sqrt{2}}\right)^2 - \left(x_2 - \frac{1}{\sqrt{2}}\right)^2 \right]$ $y_2(\mathbf{x}) = 1 - \exp \left[-\left(x_1 + \frac{1}{\sqrt{2}}\right)^2 - \left(x_2 + \frac{1}{\sqrt{2}}\right)^2 \right]$	$m = 3$ $c_1(\mathbf{x}) = x_1^2 + x_2^2 - \frac{1}{2}$ $c_2(\mathbf{x}) = \min[\{y_1(\mathbf{x}) - .4, .6 - y_1(\mathbf{x})\}]$ $c_3(\mathbf{x}) = \min[\{y_2(\mathbf{x}) - .4, .6 - y_2(\mathbf{x})\}]$	$x_1 \in [.25, 1]$ $x_2 \in [.25, 1]$	10	(1, 1)	$\mathbf{w} = (1, 2, 1)$ $\epsilon = 1$ $\gamma = 10$ $\sigma_{\text{ref}} = 1$
CIR (proposed by us)	$d = 2$ $x_1 \in [-2, 2]$ $x_2 \in [-2, 2]$	$n = 2$ $y_1(\mathbf{x}) = -\left(\frac{1}{2}\Theta[x_2 - x_1] + x_1\right)^2$ $y_2(\mathbf{x}) = -\left(\frac{1}{2}\Theta[x_1 - x_2] + x_2\right)^2$	$m = 1$ $c_1(\mathbf{x}) = \min[\{(x_1 - 1)^2 + x_2^2 - 0.25, \dots$ $\dots x_1^2 + (x_2 - 1)^2 - 0.25\}]$	$x_1 \in [.5, 1.5]$ $x_2 \in [-.5, .5]$	10	(0, 0)	$\mathbf{w} = (1, 1, 1)$ $\epsilon = 1$ $\gamma = 1$ $\sigma_{\text{ref}} = 1$

Table II: Benchmark results for 50 independent optimization runs with the notation from section III-A for the test problems from Tab. I.

Problem name	Total number of evaluations $N^\delta(\mathcal{O}, \text{adaptive-1}, \delta v)$				Break-even simulation times $\tau(\mathcal{O}, \text{adaptive-1}, \text{nsgaii}, \delta v)$			
	$\delta v = 0.80$	$\delta v = 0.85$	$\delta v = 0.90$	$\delta v = 0.95$	$\delta v = 0.80$	$\delta v = 0.85$	$\delta v = 0.90$	$\delta v = 0.95$
BNH	16.36 \pm 2.54	18.82 \pm 2.56	25.14 \pm 4.89	38.30 \pm 5.40	(0.13 \pm 0.08) s	(0.16 \pm 0.08) s	(0.22 \pm 0.10) s	(0.30 \pm 0.09) s
SRN	28.77 \pm 23.26	31.77 \pm 23.08	38.86 \pm 22.54	62.40 \pm 15.71	(0.26 \pm 0.20) s	(0.25 \pm 0.16) s	(0.24 \pm 0.12) s	(0.34 \pm 0.13) s
OSY	334.92 \pm 121.41	556.11 \pm 172.00	710.00 \pm 112.00	> 750	(1.49 \pm 1.34) s	(2.91 \pm 2.37) s	(2.83 \pm 1.56) s	–
CEX	57.82 \pm 41.50	68.31 \pm 42.04	84.81 \pm 37.48	135.87 \pm 37.88	(0.65 \pm 0.76) s	(0.52 \pm 0.52) s	(0.45 \pm 0.33) s	(0.50 \pm 0.28) s
FFF	46.29 \pm 24.81	53.87 \pm 27.50	70.53 \pm 26.49	117.13 \pm 20.78	(1.09 \pm 1.17) s	(0.97 \pm 1.19) s	(1.00 \pm 1.02) s	(2.41 \pm 1.05) s
CIR	74.04 \pm 13.49	86.20 \pm 14.22	108.09 \pm 17.41	182.45 \pm 15.37	(0.46 \pm 0.23) s	(0.44 \pm 0.21) s	(0.42 \pm 0.22) s	(0.48 \pm 0.16) s

iterations, the total effective runtime of the algorithm is given by

$$T_{\text{eff}}(\text{alg}, N_{\text{sim}}, T_{\text{sim}}) \equiv T_{\text{sim}} \left[\frac{N_{\text{seq}}(\text{alg})}{N_{\text{sim}}} \right] N_{\text{iter}}(\text{alg}) + T(\text{alg}). \quad (29)$$

3) *Break-even point:* The break-even simulation time between two competing algorithms $\text{adaptive-}N_{\text{seq}}$ and nsgaii represents the minimum value of T_{sim} for which $\text{adaptive-}N_{\text{seq}}$ has a lower total effective runtime than nsgaii . For this purpose, we count the total number of iterations $N_{\text{iter}}^\delta(\mathcal{O}, \text{alg}, \delta v)$ and the cumulated pure runtime $T^\delta(\mathcal{O}, \text{alg}, \delta v)$ (excluding the simulation time) of each algorithm to reach a certain Pareto approximation quality

$$\Delta V(\mathcal{O}, \mathbf{y}_{\text{ref}}, \text{alg}) \geq \delta v \quad (30)$$

for a given relative total dominated volume $\delta v \in [0, 1]$. This condition represents the stopping criterion **STOP(D)** for our method, cf. Alg. 1.

If each algorithm suggests sequences of $N_{\text{seq}}(\text{alg})$ design points for each of $N_{\text{iter}}^\delta(\mathcal{O}, \text{alg}, \delta v)$ iterations until this stopping criterion is reached and we set the number of parallelized simulation runs to $N_{\text{sim}} = 1$, then the break-even simulation time is given by

$$T_{\text{sim}} > \tau(\mathcal{O}, \text{adaptive-}N_{\text{seq}}, \text{nsgaii}, \delta v) \equiv \frac{T^\delta(\mathcal{O}, \text{adaptive-}N_{\text{seq}}, \delta v) - T^\delta(\mathcal{O}, \text{nsgaii}, \delta v)}{v^\delta(\text{nsgaii}) - v^\delta(\text{adaptive-}N_{\text{seq}})} \quad (31)$$

with

$$v^\delta(\text{alg}) \equiv N_{\text{seq}}(\text{alg}) \times N_{\text{iter}}^\delta(\mathcal{O}, \text{alg}, \delta v). \quad (32)$$

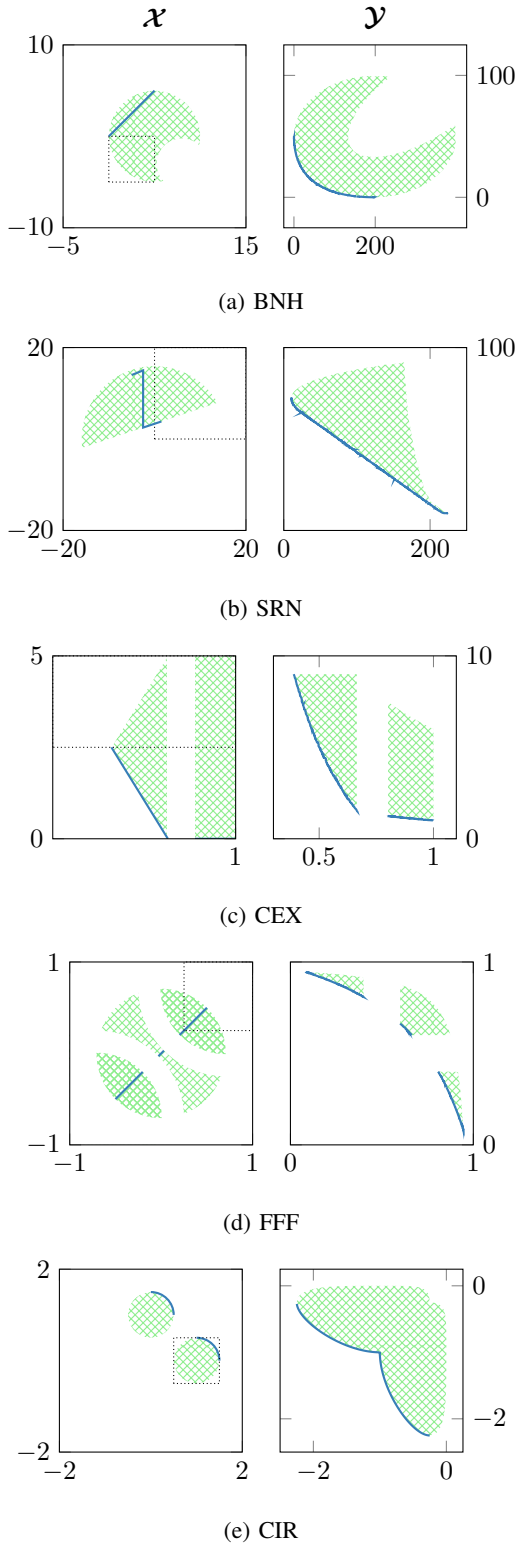


Figure 2: Sketches of five of the six test problems defined in Tab. I. For each problem, we show the design space \mathcal{X} on the left and the objective space \mathcal{Y} (together with its surrounding area) on the right with the following symbols: true feasible region, — true Pareto frontier, and border of \mathcal{X}_0 .

Here we have assumed that `adaptive- N_{seq}` has a longer cumulated pure runtime, but a smaller value of $\nu^\delta(\text{alg})$ than `nsgaii`, which holds true in practice.

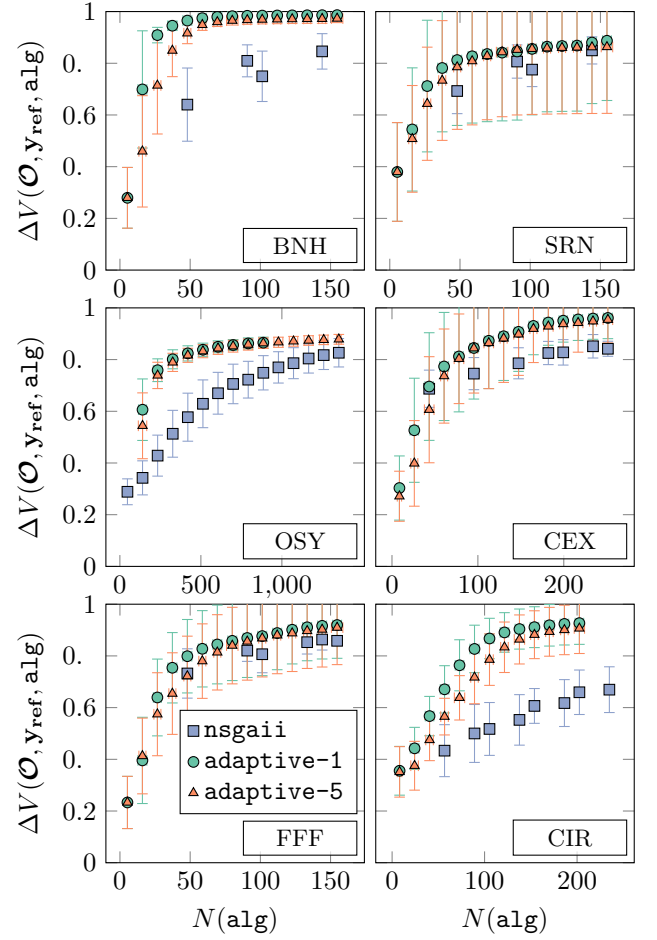


Figure 3: Relative total dominated volume $\Delta V(\mathcal{O}, \mathbf{y}_{\text{ref}}, \text{alg})$, (28), versus number of evaluated data points $N(\text{alg})$ of different algorithms `alg`. Each subplot corresponds to a different test problem \mathcal{O} from Tab. I solved with 50 independent runs. Steeper curves represent more effective optimization strategies.

B. Results

For each test problem from Tab. I we run each algorithm 50 times independently with different random seeds and evaluate the metrics discussed in section III-A. For our proposed method we use the implementation from [6] together with machine learning components from [16] and optimizers from [17], whereas for the evolutionary algorithm we use the implementation from [18].

In Tab. II we list the resulting total number of evaluations $N^\delta(\mathcal{O}, \text{adaptive-1}, \delta v)$ to reach the relative total dominated volume δv and the break-even simulation times $\tau(\mathcal{O}, \text{adaptive-1}, \text{nsgaii}, \delta v)$ for which `adaptive-1` runs faster than `nsgaii`. The table shows the mean values together with the respective standard deviations, where we make use of Gaussian error propagation for the deviations of τ . For all test problems but the high-dimensional OSY we

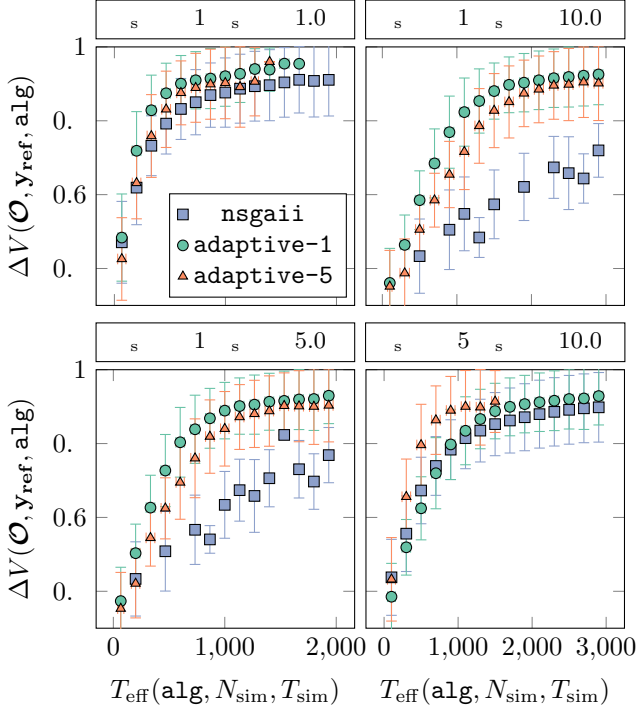


Figure 4: Relative total dominated volume $\Delta V(\mathcal{M}, \mathbf{y}_{\text{ref}}, \text{alg})$, (28), versus total effective runtimes $T_{\text{eff}}(\text{alg}, N_{\text{sim}}, T_{\text{sim}})$, (29), of different algorithms alg for the test problem CIR from Tab. I solved with 50 independent runs. In each subplot we assume a fixed number of simulation parallelizations N_{sim} and a fixed simulation evaluation time T_{sim} . Steeper curves represent faster optimization strategies.

achieve to obtain a relative dominated volume of $\delta v = 0.95$ with less than 200 evaluations. Furthermore, the break-even simulation times are all of the order of seconds, even when we include the error interval of one standard deviation.

In Fig. 3 we show the number of evaluations $N(\text{alg})$ that are required to reach a certain relative dominated volume $\Delta V(\mathcal{M}, \mathbf{y}_{\text{ref}}, \text{alg})$. We plot mean values with error bars for the standard deviations, a steeper curve represents a more effective optimization strategy. We find that our algorithm is superior to the nsgaii approach. It also becomes apparent that adaptive-1 is slightly better than adaptive-5, which means that a larger sequence of suggestions N_{seq} reduces the optimization quality. This is no surprise since further suggestions in the sequence beyond the first have to be made without additional information from evaluations.

However, longer sequence lengths allow to reduce the optimization time as we demonstrate in Fig. 4. Here we show the total effective runtimes $T_{\text{eff}}(\text{alg}, N_{\text{sim}}, T_{\text{sim}})$ that are required to reach a certain relative dominated volume $\Delta V(\mathcal{M}, \mathbf{y}_{\text{ref}}, \text{alg})$ on the test problem CIR for different numbers of simulation parallelizations N_{sim} and different simulation evaluation times T_{sim} . Clearly, for $N_{\text{sim}} = 5$, adaptive-5 is faster than adaptive-1 because its whole sequence of suggestions can be evaluated in parallel.

Finally, we explicitly show different sampling stages (20,

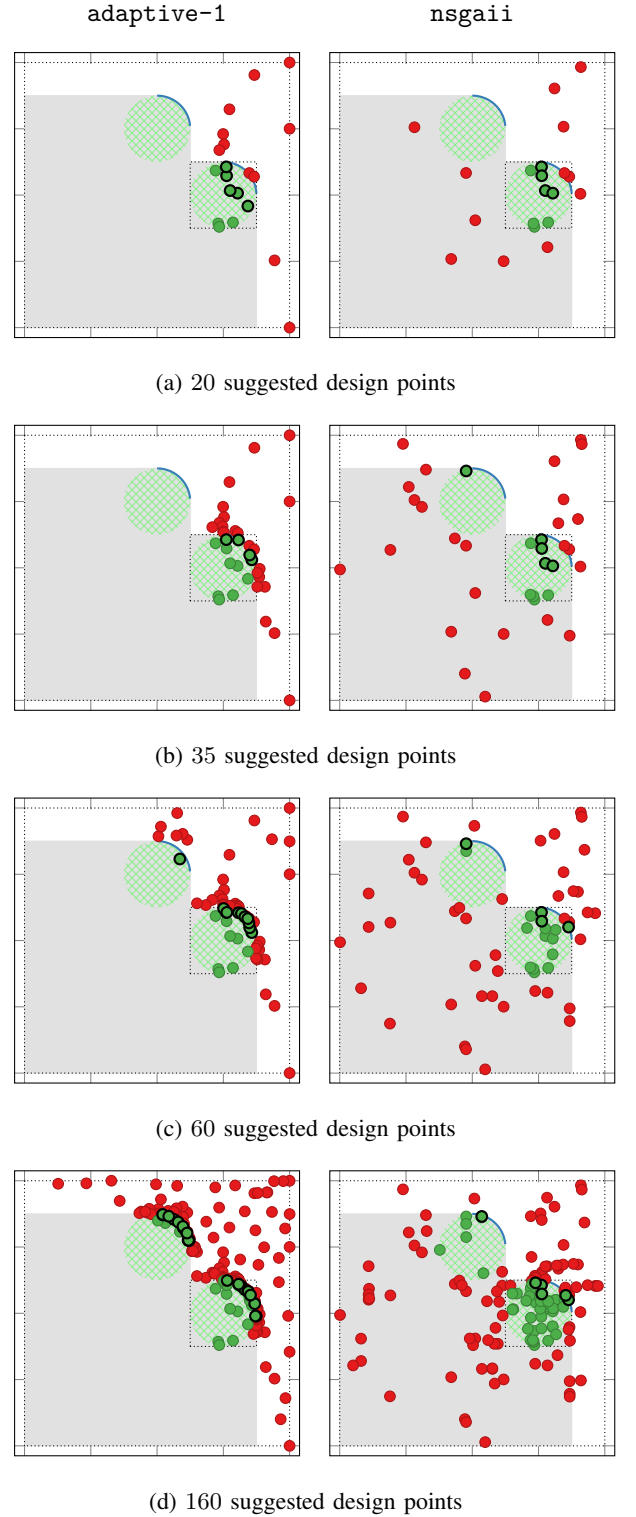


Figure 5: Exemplary visualization of different sampling stages for the test problem CIR from Tab. I based on the sketch from Fig. 2e with the following symbols: \bullet infeasible point, \bullet feasible point, \bullet Pareto optimal feasible point, --- true Pareto frontier, --- true Pareto dominated region, --- true feasible region, and --- borders of \mathcal{X}_0 and \mathcal{X} . Both algorithms start with the same set of initial points. Clearly, adaptive-1 (left) chooses the data points more efficiently than nsgaii (right) while still maintaining an explorative behavior.

35, 60, and 160 suggested points) for a single optimization run on the test problem CIR in Fig. 5. We find that `adaptive-1` achieves a much more efficient sampling which avoids Pareto dominated areas while maintaining an explorative behavior. This observation can already be made with a few samples, but becomes more and more obvious as the sampling progresses.

IV. CONCLUSION

Summarized, we have presented a novel adaptive optimization algorithm on the foundation of Bayes optimization, which allows us to solve black-box multi-objective optimization problems with binary constraints. The weight-based utility function is intuitively understandable and can be tuned to the demands of the problems at hand. Our approach is based on probabilistic regression and classification models to predict the values and feasibility of the optimization objectives. Furthermore, we have made use of a novel ellipsoid truncation method to speed up our algorithm in a straightforward way. A benchmark has shown that our approach can compete with an evolutionary algorithm on a set of test problems with respect to the number of iterations and the calculation time.

In principle, our approach could also be used to optimize noisy simulations, which would require an appropriate modification of the machine learning models. Moreover, it could also be used to handle integer design variables, which would allow us to solve integer programming problems and mixed-integer programming problems. For this purpose, both the models and the optimization of the utility function had to be adapted accordingly. Another possible improvement would be the use of explicitly calculated gradients, which could greatly improve the performance of the optimization steps. All of these conceptional ideas could serve as a promising point of origin for further studies.

ACKNOWLEDGMENT

We have realized our benchmark results with the help of [16]–[18]. This work was developed in the Fraunhofer Cluster of Excellence “Cognitive Internet Technologies”.

REFERENCES

- [1] P. I. Frazier. (2018) A tutorial on bayesian optimization. arXiv. [Online]. Available: <https://arxiv.org/abs/1807.02811>
- [2] M. Abdolshah, A. Shilton, S. Rana, S. Gupta, and S. Venkatesh, “Expected hypervolume improvement with constraints,” in *2018 24th International Conference on Pattern Recognition (ICPR)*, 2018, pp. 3238–3243.
- [3] K. Miettinen, *Nonlinear Multiobjective Optimization*, ser. International series in operations research & management science. Kluwer Academic Publishers, Dordrecht, 2004.
- [4] R. Calandra, J. Peters, and D. M.P., “Pareto front modeling for sensitivity analysis in multi-objective bayesian optimization,” in *NIPS Workshop on Bayesian Optimization 2014*, 2014.
- [5] R. Heese, M. Walczak, T. Seidel, N. Aspiron, and M. Bortz, “Optimized data exploration applied to the simulation of a chemical process,” *Computers & Chemical Engineering*, vol. 124, pp. 326–342, 2019.
- [6] R. Heese. (2020) Python implementation of Adaptive Sampling of Pareto Frontiers with Binary Constraints Using Regression and Classification. GitHub repository. [Online]. Available: <https://github.com/RaoulHeese/adasamp-pareto>
- [7] T. T. Binh and U. Korn, “Mobes: A multiobjective evolution strategy for constrained optimization problems,” in *The Third International Conference on Genetic Algorithms (Mendel 97)*, vol. 25, 1997, pp. 176–182.

- [8] V. Chankong and Y. Y. Haimes, *Multiobjective decision making: theory and methodology*. Courier Dover Publications, 2008.
- [9] A. Osyczka and S. Kundu, “A new method to solve generalized multicriteria optimization problems using the simple genetic algorithm,” *Structural optimization*, vol. 10, no. 2, pp. 94–99, 10 1995.
- [10] C. M. Fonseca and P. J. Fleming, “An overview of evolutionary algorithms in multiobjective optimization,” *Evolutionary Computation*, vol. 3, no. 1, pp. 1–16, 1995.
- [11] K. Deb, *Multi-Objective Optimization using Evolutionary Algorithms*, ser. Wiley Interscience Series in Systems and Optimization. Wiley, 2001.
- [12] K. Deb, A. Pratap, S. Agarwal, and T. Meyarivan, “A fast and elitist multiobjective genetic algorithm: Nsga-ii,” *IEEE Transactions on Evolutionary Computation*, vol. 6, no. 2, pp. 182–197, 2002.
- [13] B. Schölkopf, “The kernel trick for distances,” in *Advances in Neural Information Processing Systems 13*, T. K. Leen, T. G. Dietterich, and V. Tresp, Eds. MIT Press, 2001, pp. 301–307.
- [14] R. Storn and K. Price, “Differential evolution – a simple and efficient heuristic for global optimization over continuous spaces,” *J. of Global Optimization*, vol. 11, no. 4, pp. 341–359, 12 1997.
- [15] R. H. Byrd, P. Lu, J. Nocedal, and C. Zhu, “A limited-memory algorithm for bound-constrained optimization,” *SIAM J. Sci. Comput.*, vol. 16, no. 5, pp. 1190–1208, 1995.
- [16] F. Pedregosa, G. Varoquaux, A. Gramfort, V. Michel, B. Thirion, O. Grisel, M. Blondel, P. Prettenhofer, R. Weiss, V. Dubourg, J. Vanderplas, A. Passos, D. Cournapeau, M. Brucher, M. Perrot, and E. Duchesnay, “Scikit-learn: Machine Learning in Python,” *Journal of Machine Learning Research*, vol. 12, pp. 2825–2830, 2011.
- [17] P. Virtanen, R. Gommers, T. E. Oliphant, M. Haberland, T. Reddy, D. Cournapeau, E. Burovski, P. Peterson, W. Weckesser, J. Bright, S. J. van der Walt, M. Brett, J. Wilson, K. Jarrod Millman, N. Mayorov, A. R. J. Nelson, E. Jones, R. Kern, E. Larson, C. Carey, Í. Polat, Y. Feng, E. W. Moore, J. VanderPlas, D. Laxalde, J. Perktold, R. Cimman, I. Henriksen, E. A. Quintero, C. R. Harris, A. M. Archibald, A. H. Ribeiro, F. Pedregosa, P. van Mulbregt, and S. Contributors, “SciPy 1.0: Fundamental Algorithms for Scientific Computing in Python,” *Nature Methods*, vol. 17, pp. 261–272, 2020.
- [18] D. Hadka. (2019) Platypus – A Free and Open Source Python Library for Multiobjective Optimization. GitHub repository. [Online]. Available: <https://github.com/Project-Platypus/Platypus>
- [19] J.-W. K. Michael Emmerich, André Deutz. (2008, 09) The computation of the expected improvement in dominated hypervolume of pareto front approximations. [Online]. Available: <http://liacs.leidenuniv.nl/~emmerichmtm/moda/material/TR-ExI.pdf>
- [20] K. Dächert, K. Klamroth, R. Lacour, and D. Vanderpooten, “Efficient computation of the search region in multi-objective optimization,” *European Journal of Operational Research*, vol. 260, no. 3, pp. 841–855, 2017.
- [21] K. Yang, M. Emmerich, A. Deutz, and T. Bäck, “Efficient computation of expected hypervolume improvement using box decomposition algorithms,” *Journal of Global Optimization*, vol. 75, no. 1, pp. 3–34, 9 2019.
- [22] M. T. M. Emmerich, “Single- and multi-objective evolutionary design optimization assisted by gaussian random field metamodels,” dissertation, Universität Dortmund, 2005.

APPENDIX

A. Expected hypervolume improvement

In this section, we outline the calculation of (12). Specifically, we use a straightforward approach along the lines of [19] with calculation time of order $O(|\mathbf{P}(\mathbf{D}_y^*)|^d)$. There are various approaches to speed up the calculation, see e.g., [20], [21].

As sketched in Fig. 6, we define the expected hypervolume improvement

$$\begin{aligned} \text{EVI}(\mathbf{D}_{\mathbf{xy}}^*, \mathbf{y}_{\text{ref}}; \mathbf{x}) &= \int_{-\infty}^{+\infty} \sum_{\mathbf{s} \in \mathbf{S}_{\mathcal{Z}}(\mathbf{D}_{\mathbf{y}}^*, \mathbf{y}_{\text{ref}})} \hat{p}_{\mathbf{y}}(\mathbf{y} | \mathbf{D}_{\mathbf{xy}}^*, \mathbf{x}) \\ &\quad \times \Delta V(\mathbf{s}, \mathbf{S}_{\mathcal{Z}}(\mathbf{D}_{\mathbf{y}}^*, \mathbf{y}_{\text{ref}}); \mathbf{y}) d\mathbf{y} \quad (33) \end{aligned}$$

locally on a non-regular grid of sectors

$$\begin{aligned} \mathbf{S}(\mathbf{D}_{\mathbf{y}}^*, \mathbf{y}_{\text{ref}}) \equiv & \left\{ \mathbf{s} = ((y_1^{j_1}, y_1^{j_2}), \dots, (y_n^{j_n}, y_n^{j_{n+1}})) \in \Xi \mid \right. \\ & y_i^{j_i} = \begin{cases} y_{\text{ref } i} & \text{if } j_i = 0 \\ -\infty & \text{if } j_i > |\mathbf{P}(\mathbf{D}_{\mathbf{y}}^*)| \\ y_i \in \mathbf{P}(\mathbf{D}_{\mathbf{y}}^*) & \text{else} \end{cases} \left. \right\} \\ & \forall j_i \in \{0, \dots, |\mathbf{P}(\mathbf{D}_{\mathbf{y}}^*)| + 1\} \\ & \forall i = 1, \dots, n \\ & \wedge y_i^{j_{i-1}} \geq y_i^{j_i} \geq y_i^{j_{i+1}} \\ & \forall j_i \in \{1, \dots, |\mathbf{P}(\mathbf{D}_{\mathbf{y}}^*)|\} \\ & \forall i = 1, \dots, n \}. \end{aligned} \quad (34)$$

Each grid sector is defined as a tuple of corner points $(y_1^{j_1}, y_1^{j_2}), \dots, (y_n^{j_n}, y_n^{j_{n+1}})$ from the set of possible grid points

$$\Xi \equiv \xi_1^2 \times \dots \times \xi_n^2, \quad (35)$$

where

$$\begin{aligned} \xi_i \equiv & \{y_i \in \mathbb{R} \cup \{-\infty\} \mid \mathbf{y} \in \mathbf{P}(\mathbf{D}_{\mathbf{y}}^*) \cup \{\mathbf{y}_{\text{ref}}, -\infty\}\} \\ & \forall i = 1 \dots n. \end{aligned} \quad (36)$$

For convenience we use $-\infty$ to denote a vector whose entries are all negative infinity. The grid expands from this symbolic point to the reference point \mathbf{y}_{ref} , (15).

Furthermore, we have made use of the subset

$$\begin{aligned} \mathbf{S}_{\neq}(\mathbf{D}_{\mathbf{y}}^*, \mathbf{y}_{\text{ref}}) \equiv & \left\{ \mathbf{s} = ((y_1^{j_1}, y_1^{j_2}), \dots, (y_n^{j_n}, y_n^{j_{n+1}})) \in \Xi \mid \right. \\ & \mathbf{s} \in \mathbf{S}(\mathbf{D}_{\mathbf{y}}^*, \mathbf{y}_{\text{ref}}) \\ & \wedge \forall \mathbf{y} \in \mathbf{P}(\mathbf{D}_{\mathbf{y}}^*) \exists i : y_i^{j_i} < y_i \left. \right\} \end{aligned} \quad (37)$$

of non-dominated grid sectors of $\mathbf{S}(\mathbf{D}_{\mathbf{y}}^*, \mathbf{y}_{\text{ref}})$ and the local volume integrand

$$\Delta V(\mathbf{s}, \mathbf{S}; \mathbf{y}) \equiv \sum_{\bar{\mathbf{s}} \in \mathbf{S}_{\mathbf{L}}(\mathbf{s}, \mathbf{S})} \prod_{i=1}^n (y_i - \delta_{\bar{y}_i^{j_i}, y_i^{j_i}} \bar{y}_i^{j_{i+1}}) \mathbb{1}_V(\mathbf{s}; \mathbf{y}) \quad (38)$$

with the indicator function

$$\mathbb{1}_V(\mathbf{s}; \mathbf{y}) \equiv \begin{cases} 1 & \text{if } y_i^{j_{i+1}} \leq y_i \leq y_i^{j_i} \forall i \\ 0 & \text{otherwise} \end{cases} \quad (39)$$

as well as the set of local sectors

$$\begin{aligned} \mathbf{S}_{\mathbf{L}}(\mathbf{s}, \mathbf{S}) \equiv & \left\{ \bar{\mathbf{s}} = ((\bar{y}_1^{j_1}, \bar{y}_1^{j_2}), \dots, (\bar{y}_n^{j_n}, \bar{y}_n^{j_{n+1}})) \in \Xi \mid \bar{\mathbf{s}} \in \mathbf{S} \right. \\ & \wedge \exists i : \bar{y}_i^{j_i} \geq y_i^{j_i} \\ & \left. \text{with } \mathbf{s} = ((y_1^{j_1}, y_1^{j_2}), \dots, (y_n^{j_n}, y_n^{j_{n+1}})) \right\}, \end{aligned} \quad (40)$$

which is a subset of \mathbf{S} .

For a regression model, (6a), with separable probabilities

$$\hat{p}_{\mathbf{y}}(\mathbf{y} | \mathbf{D}_{\mathbf{xy}}^*, \mathbf{x}) = \prod_{i=1}^n \hat{p}_{y_i}(y_i | \mathbf{D}_{\mathbf{xy}}^*, \mathbf{x}) \quad (41)$$

we can interchange the integral and sums in (33) due to Tonelli's theorem and arrive at

$$\begin{aligned} \text{EVI}(\mathbf{D}_{\mathbf{xy}}^*, \mathbf{y}_{\text{ref}}; \mathbf{x}) = & \sum_{\mathbf{s} \in \mathbf{S}_{\neq}(\mathbf{D}_{\mathbf{y}}^*, \mathbf{y}_{\text{ref}})} \sum_{\bar{\mathbf{s}} \in \mathbf{S}_{\mathbf{L}}(\mathbf{s}, \mathbf{S}_{\neq}(\mathbf{D}_{\mathbf{y}}^*, \mathbf{y}_{\text{ref}}))} \\ & \times \prod_{i=1}^n \int_{y_i^{j_{i+1}}}^{y_i^{j_i}} (y_i - \delta_{\bar{y}_i^{j_i}, y_i^{j_i}} \bar{y}_i^{j_{i+1}}) \hat{p}_{y_i}(y_i | \mathbf{D}_{\mathbf{xy}}^*, \mathbf{x}) dy_i. \end{aligned} \quad (42)$$

In case of normal probability densities

$$\hat{p}_{y_i}(y_i | \mathbf{D}_{\mathbf{xy}}^*, \mathbf{x}) = \mathcal{N}(y_i | \mu_i(\mathbf{D}_{\mathbf{xy}}^*, \mathbf{x}), \sigma_i^2(\mathbf{D}_{\mathbf{xy}}^*, \mathbf{x})) \quad (43)$$

with mean $\mu_i(\mathbf{D}_{\mathbf{xy}}^*, \mathbf{x}) \equiv \mu_i$ and standard deviation $\sigma_i(\mathbf{D}_{\mathbf{xy}}^*, \mathbf{x}) \equiv \sigma_i$ for $i = 1, \dots, n$, this expression can be straightforwardly written in a closed form using exponential and error functions. The closed form contains only three different types of integrals I_1 , I_2 , and I_3 with

$$\begin{aligned} I_1(a, b, c; \mu, \sigma) \equiv & \int_a^b (y - c) \mathcal{N}(y | \mu, \sigma^2) dy \\ = & \frac{\mu - c}{2} \left[\text{erf}\left(\frac{b - \mu}{\sqrt{2}\sigma}\right) - \text{erf}\left(\frac{a - \mu}{\sqrt{2}\sigma}\right) \right] \\ & + \frac{\sigma}{\sqrt{2\pi}} \left[\exp\left(-\frac{(a - \mu)^2}{2\sigma^2}\right) - \exp\left(-\frac{(b - \mu)^2}{2\sigma^2}\right) \right], \end{aligned} \quad (44a)$$

$$\begin{aligned} I_2(b, c; \mu, \sigma) \equiv & \int_{-\infty}^b (y - c) \mathcal{N}(y | \mu, \sigma^2) dy \\ = & \frac{\mu - c}{2} \left[\text{erf}\left(\frac{b - \mu}{\sqrt{2}\sigma}\right) + 1 \right] \\ & + \frac{\sigma}{\sqrt{2\pi}} \exp\left(-\frac{(b - \mu)^2}{2\sigma^2}\right), \end{aligned} \quad (44b)$$

and

$$\begin{aligned} I_3(a, b; \mu, \sigma) \equiv & \int_a^b y \mathcal{N}(y | \mu, \sigma^2) dy \\ = & \frac{1}{2} \left[\text{erf}\left(\frac{b - \mu}{\sqrt{2}\sigma}\right) - \text{erf}\left(\frac{a - \mu}{\sqrt{2}\sigma}\right) \right], \end{aligned} \quad (44c)$$

respectively. Here we have used the abbreviations $\mu \in \{\mu_1, \dots, \mu_n\}$, $\sigma \in \{\sigma_1, \dots, \sigma_n\}$, and $a, b, c \in \xi_i \setminus \{-\infty\} \forall i = 1, \dots, n$.

In practice, the standard deviations σ_i can become smaller than the numerical precision. In this case, the limit

$$\mathcal{N}(y_i | \mu_i, \sigma_i^2) \xrightarrow{\sigma_i \rightarrow 0} \delta(y_i - \mu_i) \quad (45)$$

with the Dirac delta distribution δ can be used to obtain

$$I_1(a, b, c; \mu, \sigma) \xrightarrow{\sigma \rightarrow 0} (\mu - c) \Theta[b - \mu] \Theta[\mu - a], \quad (46a)$$

$$I_2(b, c; \mu, \sigma) \xrightarrow{\sigma \rightarrow 0} (\mu - c) \Theta[b - \mu], \quad (46b)$$

and

$$I_3(a, b; \mu, \sigma) \xrightarrow{\sigma \rightarrow 0} \Theta[b - \mu] \Theta[\mu - a], \quad (46c)$$

respectively, where Θ denotes the Heaviside theta function.

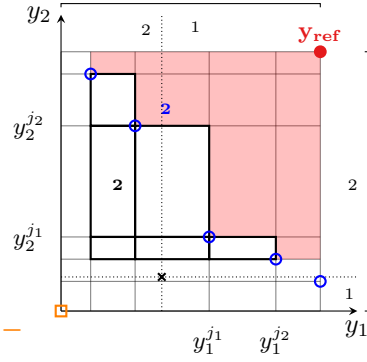


Figure 6: Expected hypervolume improvement sketch ($n = 2$) for appendix A with the following symbols: \circ Pareto optimal solutions, \bullet reference point \mathbf{y}_{ref} , \square symbolic point in negative infinity $-\infty$, \times means μ_1 and μ_2 of the regression model probability density intersecting at \mathbf{x} , and red shaded region Pareto dominated region.

B. Ellipsoid truncation method

In this section, we outline the expected hypervolume approximation used in (24), which is applicable for a regression model with a normal and separable probability density, (6a), (41) and (43), with means μ_1, \dots, μ_n and standard deviations $\sigma_1, \dots, \sigma_n$. As sketched in Fig. 7, the basic idea is to neglect sectors in (42) which do not intersect with an ellipse of a given size corresponding to the probability density function so that

$$\text{EVI}(\mathbf{D}_{\mathbf{xy}}^*, \mathbf{y}_{\text{ref}}; \mathbf{x}) \approx \widehat{\text{EVI}}(\mathbf{D}_{\mathbf{xy}}^*, \mathbf{y}_{\text{ref}}, \sigma_{\text{ref}}; \mathbf{x}) \equiv \sum_{\mathbf{s} \in \tilde{\mathbf{S}}_{\mathbf{x}}(\mathbf{D}_{\mathbf{y}}^*, \mathbf{y}_{\text{ref}}, \sigma_{\text{ref}}; \mathbf{x})} \dots \quad (47)$$

with the subset

$$\begin{aligned} \tilde{\mathbf{S}}_{\mathbf{x}}(\mathbf{D}_{\mathbf{y}}^*, \mathbf{y}_{\text{ref}}, \sigma_{\text{ref}}; \mathbf{x}) \equiv & \left\{ \mathbf{s} = ((y_1^{j_1}, y_1^{j_2}), \dots, (y_n^{j_n}, y_n^{j_{n+1}})) \right. \\ & \in \Xi \mid \mathbf{s} \in \mathbf{S}_{\mathbf{x}}(\mathbf{D}_{\mathbf{y}}^*, \mathbf{y}_{\text{ref}}) \\ & \left. \wedge \mathbf{H}(\mathbf{s}) \cap \mathbf{E}(\mathbf{D}_{\mathbf{xy}}^*, \sigma_{\text{ref}}; \mathbf{x}) \neq \{\} \right\} \quad (48) \end{aligned}$$

of $\mathbf{S}_{\mathbf{x}}(\mathbf{D}_{\mathbf{y}}^*, \mathbf{y}_{\text{ref}})$. Here we use $\mathbf{H}(\mathbf{s})$ to denote the points contained in the n -dimensional hyperbox spanned by the points in \mathbf{s} and $\mathbf{E}(\mathbf{D}_{\mathbf{xy}}^*, \sigma_{\text{ref}}; \mathbf{x})$ to denote the points contained in the hyperellipsoid with centers μ_1, \dots, μ_n and eccentricities $\sigma_{\text{ref}}\sigma_1, \dots, \sigma_{\text{ref}}\sigma_n$, respectively.

This approximation effectively allows us to truncate the sum in (42) and therefore skip the calculation of the corresponding integrals which have a neglectable effect on the outcome.

C. Probability of being non-dominated

In this section, we outline the calculation of (18). Similar calculations can also be found in [22]. For a regression model with separable probabilities, (6a) and (41), we can write

$$\begin{aligned} p_{\mathbf{x}}(\mathbf{D}_{\mathbf{xy}}^*; \mathbf{x}) &= p(\forall \mathbf{y} \in \mathbf{D}_{\mathbf{y}}^* \exists i : \hat{y}_i(\mathbf{D}_{\mathbf{xy}}^*; \mathbf{x}) > y_i) \\ &= \prod_{\mathbf{y} \in \mathbf{D}_{\mathbf{y}}^*} \sum_I \left[\prod_{l \in I} p(\hat{y}_l(\mathbf{D}_{\mathbf{xy}}^*; \mathbf{x}) > y_l) \right. \\ &\quad \left. \prod_{l \notin I} p(\hat{y}_l(\mathbf{D}_{\mathbf{xy}}^*; \mathbf{x}) \leq y_l) \right] \quad (49) \end{aligned}$$

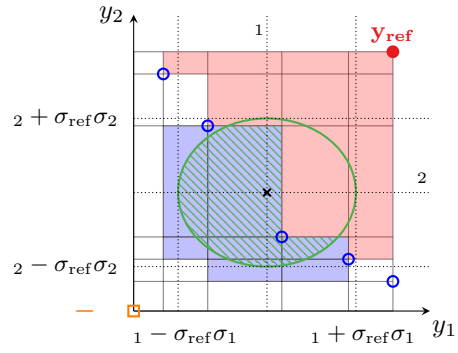


Figure 7: Ellipsoid truncation method sketch ($n = 2$) for appendix B with the symbols from Fig. 6 and the additional symbols: $\text{blue shaded region}$ non-truncated areas, which partially overlap with the green ellipse truncation ellipse.

with I representing all possible combination of index sets of $\{1, \dots, n\}$ with at least one element. Equation (49) can also be written as

$$p_{\mathbf{x}}(\mathbf{D}_{\mathbf{xy}}^*; \mathbf{x}) = \prod_{\mathbf{y} \in P(\mathbf{D}_{\mathbf{y}}^*)} \sum_{b \in B} \prod_{l=1}^n p_{\mathbf{x}}^{b_l}(\mathbf{D}_{\mathbf{xy}}^*; \mathbf{y}, \mathbf{x}). \quad (50)$$

Here we have introduced

$$p_{\mathbf{x}}^{b_l}(\mathbf{D}_{\mathbf{xy}}^*; \mathbf{y}, \mathbf{x}) \equiv \begin{cases} \int_{-\infty}^{y_l} \hat{p}_{y_l}(y_l | \mathbf{D}_{\mathbf{xy}}^*, \mathbf{x}) & \text{if } b_l = 0 \\ \int_{y_l}^{+\infty} \hat{p}_{y_l}(y_l | \mathbf{D}_{\mathbf{xy}}^*, \mathbf{x}) & \text{else} \end{cases} \quad (51)$$

and

$$\mathbf{y}_{\neq i} \equiv (y_1, \dots, y_{i-1}, y_{i+1}, \dots, y_n), \quad (52)$$

and the set

$$\begin{aligned} B \equiv & \left\{ (b_1, \dots, b_n) \mid b_n \in \{0, 1\} \forall i = 1 \dots n \right. \\ & \left. \wedge \sum_{i=1}^n b_{i=1} > 0 \right\} \quad (53) \end{aligned}$$

containing all combinations of $\{0, 1\}$ of length n with repetition and with order-significance.

For a regression model with a normal probability density, (43), this expression can be straightforwardly rewritten in a closed form in terms of error functions. Specifically, one has

$$p(\hat{y}_i(\mathbf{D}_{\mathbf{xy}}^*; \mathbf{x}) \leq y_i) = \frac{1}{2} \left(1 - \text{erf} \left[\frac{\mu_i - y_i}{\sqrt{2}\sigma_i} \right] \right) \quad (54a)$$

and

$$p(\hat{y}_i(\mathbf{D}_{\mathbf{xy}}^*; \mathbf{x}) > y_i) = \frac{1}{2} \left(1 + \text{erf} \left[\frac{\mu_i - y_i}{\sqrt{2}\sigma_i} \right] \right), \quad (54b)$$

respectively. In analogy to (46), the limit (45) can be used to obtain

$$p(\hat{y}_i(\mathbf{D}_{\mathbf{xy}}^*; \mathbf{x}) \leq y_i) \xrightarrow{\sigma_i \rightarrow 0} \Theta[\mu_i - y_i] \quad (55a)$$

and

$$p(\hat{y}_i(\mathbf{D}_{\mathbf{xy}}^*; \mathbf{x}) > y_i) \xrightarrow{\sigma_i \rightarrow 0} \Theta[y_i - \mu_i] \quad (55b)$$

in case of vanishing standard deviations σ_i .